TEC3 WORK ROLL THERMAL CROWN MODEL FOR HOT AND COLD ROLLING OF STEEL *

Nicolas LEGRAND[1]
Nelson SOUTO[2]
Sami ABDELKHALEK[3]
Zafer KOONT[4]

Abstract
A work roll thermal crown model has been developed for a wide range of hot and cold rolling mill applications. The model is extremely fast, robust and accurate to determine the evolution of thermal crown all along the rolling campaigns. It has also ability to consider work roll shifting, multiple segmented cooling zones along the length and circumference of the roll as well as composite rolls properties (e.g. different thermal properties between mandrel and core of the roll). Moreover, the model includes simultaneously fast and slow temperature evolution calculations, respectively near roll surface (skin area) and at a certain distance below the roll surface (bulk area). This gives to thermal crown predictions a higher accuracy than conventional thermal crown models from literature that consider only the slow temperature evolution regime. An optimization procedure together with roll surface temperature and roll thermal profile measurements have been used to tune the model. The tuned model applied to hot rolling conditions has shown a significant influence of roll shifting and composite rolls properties on the prediction of roll temperature distribution and thermal crown during rolling. The tuned model applied to cold rolling conditions highlights the importance of mill operators practices to modify cooling distribution across roll barrel length with the segmented cooling zones to adjust the thermal crown and to get better strip shape control.
Keywords: Cold rolling; Hot rolling; Thermal crown; Composite roll.

[1] *ArcelorMittal Global R&D East Chicago, USA.*
[2] *ArcelorMittal Global R&D Maizieres, France.*
[3] *Military academy of Fondouk Jedid, 8012 Nabeul, Tunisia*
[4] *ArcelorMittal Global R&D Hamilton, Canada.*

Nomenclature

r, θ, y – radial, angular and axial roll coordinates [mm, degree, mm]
T – temperature [Celsius]
K, ρ.c – thermal conductivity, heat capacity coefficient of roll [W/m.°C, J/mm^3.°C]
$a = \frac{K}{\rho.c}$ *– thermal diffusivity* [m^2/s]
h_i, T_i, $\Delta\theta_i$ *– heat transfer coefficient, external temperature and angular portion of zone i around the roll* [W/mm^2/°C, °C, degree]
u_r *– roll radial displacement due to roll thermal expansion* [mm]
α *– roll thermal expansion coefficient [/°C]*
D, R – roll diameter, roll radius [mm]
ω *– roll angular speed [radian/sec.]*
E, υ *– roll Young's modulus and Poison ratio* [N/mm^2, no unit]
T_{eq}, T_{water}, T_s^{axi} *– steady state roll temperature, water temperature, roll surface axi-symmetric temperature* [°C]
ϕ, h' – average heat flux exchanged with roll bulk, corresponding heat transfer coefficient with bulk (TEC3 [W/m, kW/m2/K]
ψ, h'' – average heat flux provided to roll by roll bite, corresponding heat transfer coefficient (TEC3) [W/m, kW/m2/K]
C_{40}, C_{100} – roll thermal crown at 40 and 100 mm from edge. C_{40}/C_{100} = thermal expansion at center - thermal expansion at 40/100 mm from edge [mm]

* *Technical contribution to the 11th International Rolling Conference, part of the ABM Week 2019, October 1st-3rd, 2019, São Paulo, SP, Brazil.*

1. BACKGROUND – STATE OF THE ART

In hot rolling, profile and Flatness control systems in Finishing Hot Strip Mills are crucial not only to respect the tolerance of the final strip crown and flatness but also for rolling stability to maintain a good strip shape in inter-stands to avoid cobles, rolling incidents and increase mill productivity. The performance of these systems depends on the ability to calculate accurately the different contributions to the roll gap profile (roll stack deflection, roll wear, roll thermal crown, strip reaction). Among these contributions, the roll thermal expansion, object of this article, has a significant influence and requires an accurate model for roll thermal crown predictions.
In cold rolling, the prediction of thermal crown is important as well for strip shape control, though thermal crown amplitude is lower than in hot rolling.

1.1 Roll heat transfers - thermal crown

The work rolls are heated during rolling by friction, strip plastic deformation and heat conduction through the roll-strip contact in the bite. Rolls are also cooled down outside the roll bite by roll cooling headers. This generates the following heat transfers: one part of the heat flux $\boldsymbol{\psi}$ supplied to roll by the bite is extracted by roll cooling headers, air or back up rolls, while the remaining part $\boldsymbol{\phi}$ penetrates the bulk of the roll (Figure 1).

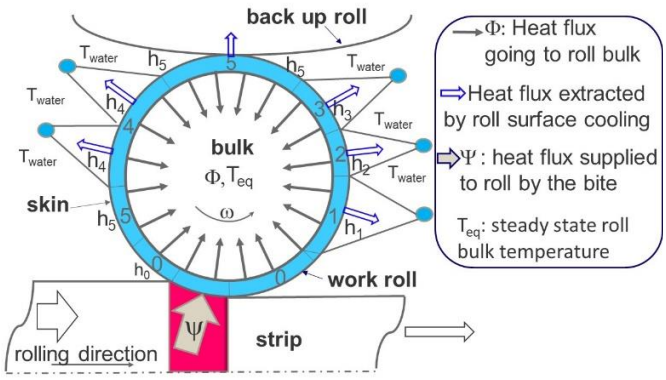

Figure 1. Heat transfers in and from the roll in the skin area (roll bite, roll cooling, air and back up roll contact) and in the bulk area.

This heat transfer $\boldsymbol{\phi}$ produces a heterogeneous temperature distribution in the bulk of the roll which results in a heterogeneous thermal expansion called *roll thermal crown.*
The knowledge of this thermal crown is crucial for mill roll gap positions settings for threading (e.g. control of thickness) or to determine optimum roll cooling and roll bending settings (e.g. control of flatness).

1.2 Existing thermal crown models

Numerous roll thermal crown models have been developed in literature for hot and cold rolling mill applications **[1-5].** These models generally calculate the work roll temperature distribution for a certain rolling and cooling condition by solving the following 2D axi-symmetric heat conduction equation:

$$\frac{\partial T}{\partial t} = a.\left[\frac{\partial^2 T}{\partial r^2} + \frac{1}{r}.\frac{\partial T}{\partial r} + \frac{\partial^2 T}{\partial z^2}\right] \quad (1)$$

Here only the bulk axi-symmetric area dealing with slow temperature evolutions in the roll is considered (Figure 1). The non axi-symmetric skin area due to the fast cyclic temperature variations at each roll revolution (Figure 1) is neglected as its contribution to thermal crown is un-significant. To solve Equation (1), thermal boundary conditions of the roll are defined by an equivalent homogeneous environment $(\bar{h}, \bar{T})$ obtained by averaging heat transfers and temperatures of the different external zones exchanging heat with the roll in rotation (Figure 2). This equivalence is defined by:

$$\bar{h} = \frac{\sum_i h_i.\Delta\theta_i}{\sum_i \Delta\theta_i} \quad (2)$$

$$\bar{T} = \frac{\sum_i T_i.h_i.\Delta\theta_i}{\sum_i h_i.\Delta\theta_i} \quad (3)$$

The above expressions are obtained by assuming that the equivalent homogeneous environment exchanges the

same amount of heat with the work roll as the sum of each individual environment[1]. However, it is not clear how accurate this equivalence $(\bar{h}, \bar{T})$ is since the model neglects the fast non axi-symmetric heat exchanges in the skin area near the roll surface (Figure 1).

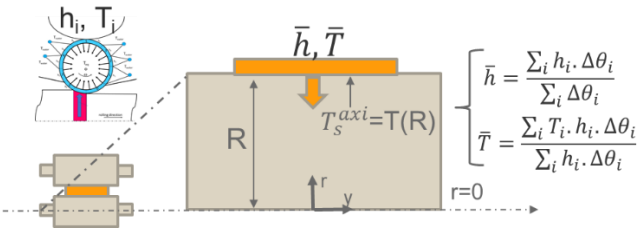

Figure 2. Existing thermal crown models based on equivalent homogeneous environment [**1-5**].

1.3 Roll thermal crown evaluations

The temperature gradients are small inside the work roll. So the roll can be considered as a set of independent rings that can thermally expand individually without interaction in between (e.g. no shear stress between rings) (Figure 3). From the temperature distribution obtained with Equation (1), the thermal crown is thus computed using an analytical 1D thermo-elastic equation in plane strain (4) **[6]** or plane stress (5) **[8]** conditions, applied on the different rings:

$$u_r = (1+\upsilon)\frac{4.\alpha}{D}\int_0^{\frac{D}{2}} \Delta T(r).r.dr \qquad (4)$$

$$u_r = \frac{4.\alpha}{D}\int_0^{\frac{D}{2}} \Delta T(r).r.dr \qquad (5)$$

Figure 3. Representation of the thermal crown calculation in **[1-5]** considering independent expansion rings

[1]Equations (2) and (3) consider only zones i outside the roll bite; the roll bite zone is not included in the average but treated separately. Moreover, in [2], $\bar{T}$ expression is more complex than in Equation (3) as it depends on rolling speed and bite friction flux.

ΔT is the local roll temperature variation from its initial temperature (ΔT=$T(r)$-$T_{initial}(r)$).
The plane strain or plane stress assumptions in Equations (4) and (5) are questionnable and must be verified here since radial and axial dimensions of the roll are of same order[2].

1.4 Composite roll properties

Work rolls, especially for hot rolling, have composite e.g. heterogeneous thermal and mechanical properties across their section (Figure 4).

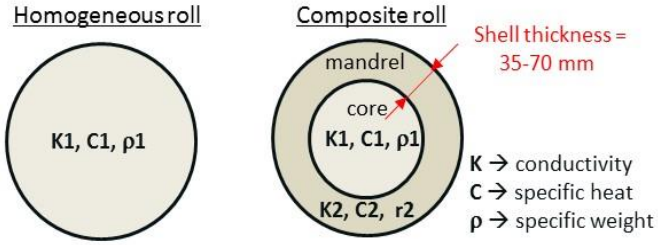

Figure 4. Illustration of homogeneous and heterogeneous (composite) roll thermal properties.

Thermal conductivity K, thermal expansion coefficient α and elasticity coefficients (E, ν) can be sometimes very different between the core and the mandrel of the roll. However, it is unclear how much these composite roll properties modify the roll thermal crown in comparison to homogeneous roll properties. Moreover, even if online thermal crown models on rolling mills generally consider these composite roll properties by type of roll grade (CPC, HiCr, ICDP …) to calculate thermal crown; they do not distinguish roll supplier, characterized by the differences of roll thermal properties between core and mandrel, which may vary even for a same type of roll grade.

[2] Indeed, to respect rigorously the plane strain or plane stress assumptions of Equation (4) and (5), the roll radial and axial dimensions should be very different in order of magnitude: for example roll radial dimension is considerably larger than roll axial dimension to satisfy the plane stress assumption, roll radial dimension is considerably lower than roll axial dimension to satisfy the plane strain assumption. However, rolls have a 500-700 mm radial dimension (diameter) and a 1500-2000 mm axial dimension, which are of similar magnitude.

1.5 Objectives of the present work

Based on the previous analysis, the present work aims at illustrating with the TEC3 thermal crown model the importance of considering both the fast and slow roll thermal regimes as well as the composite rolls properties (and their differences between roll suppliers) to predict accurately roll temperature and thermal crown during rolling. It is also shown in this work that the 2D thermo-elastic equation of TEC3 for thermal crown has a higher accuracy in comparison to the 1D literature equations.

2. TEC3 MODEL DESCRIPTION

The TEC3 thermal crown Finite Element model of the present work, initially developed by **[7]**, has ability to describe the fast temperature evolution near the roll surface in the skin area (skin mesh (r,θ)) and the slow temperature evolution in the bulk area of the roll (bulk mesh (r,y) associated with the thermal crown evolution (Figure 5). These two meshes enable the model large integration time steps so small computation time per coil (~1 sec./coil) because the steady state skin mesh needs to be refined only in the roll bite area. This makes the model suitable for online applications.

This ability for fast and slow temperature evolutions description is innovative as most literature models consider the slow temperature evolution only, added to the equivalent homogeneous environment exposed previously (see section 1.2).

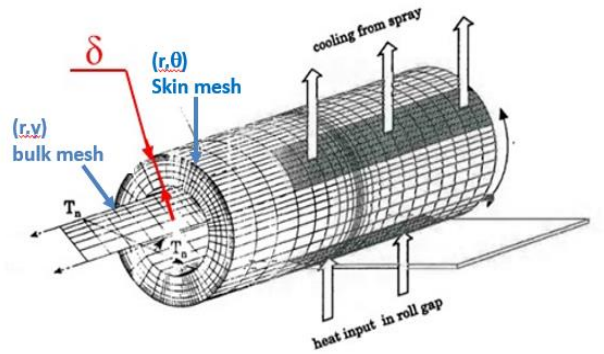

Figure 5. TEC3 thermal crown model with the two meshes.

Heat equations to calculate with TEC3 the roll temperature distribution in the roll (skin and bulk roll areas) are established below.

2.1 Roll heat conduction equations

The heat conduction and convection in cylindrical coordinates inside a roll in rotation without source term can be described by the following 3D partial differential equation:

$$\frac{\partial T}{\partial t} + \omega.\frac{\partial T}{\partial \theta} = a.\left[\frac{1}{r}.\frac{\partial}{\partial r}.\left(r.\frac{\partial T}{\partial r}\right) + \frac{1}{r^2}.\frac{\partial^2 T}{\partial \theta^2} + \frac{\partial^2 T}{\partial z^2}\right] \quad (6)$$

In the skin area, the roll surface gets cyclic temperature variations during one revolution coming from the contact with the several environments: exit, entry, lubrication cooling, roll bite, back up roll, air (Figure 1). In this skin area, the roll temperature is assumed steady state each time step (one time step ~ one roll revolution) but evolves at each time step due to modification of boundary conditions coming from the unsteady state core roll thermal crown model. So heat conduction in the roll boundary layer (skin area) is described by the following 2D steady state equation (Figure 5) where axial heat transfers are neglected:

$$\omega.\frac{\partial T}{\partial \theta} = a.\left[\frac{1}{r}.\frac{\partial}{\partial r}.\left(r.\frac{\partial T}{\partial r}\right) + \frac{1}{r^2}.\frac{\partial^2 T}{\partial \theta^2}\right] \quad (7)$$

These non axi-symmetric variations of temperature modify a small thickness of roll surface $\delta \approx 4\sqrt{a/\omega}$ (a few mm thickness), so their contribution to the thermal crown is considered negligible.

Below this small thickness δ, in the bulk area (Figure 1), axi-symmetric unsteady state thermal conditions prevail, which enables to neglect terms in θ in Equation (6) and solve the problem in 2D axisymmetric conditions (plane (r,z)). Therefore in the bulk area (Figure 6), the heat conduction Equation (6) in the roll can be reduced to the 2D axi-symmetric heat conduction equation:

$$\frac{\partial T}{\partial t} = a.\left[\frac{1}{r}.\frac{\partial}{\partial r}.\left(r.\frac{\partial T}{\partial r}\right) + \frac{\partial^2 T}{\partial y^2}\right] \quad (8)$$

This equation is the same as equivalent homogeneous environment models (Equation (1)). However here, the boundary conditions are different. They are provided by the internal surface of the skin area [h', T(R-δ)] and not by the equivalent homogeneous environment $(\bar{h}, \bar{T})$ (Equation 2 and 3).

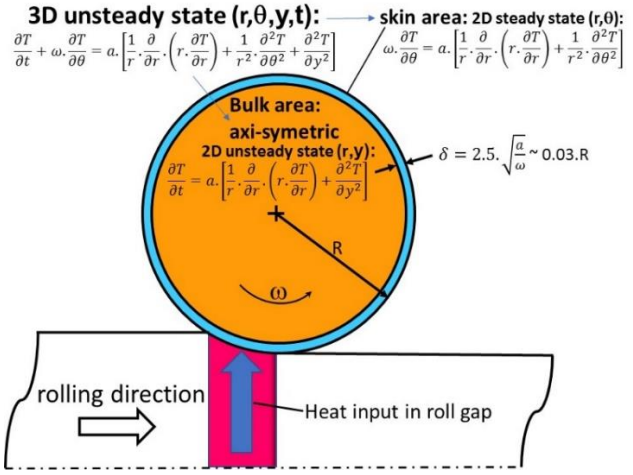

Figure 6.TEC3 thermal crown model and equations associated to fast (skin area) and slow (bulk area) temperature evolutions.
It is here pointed out that the thermal transient problem of the thermal crown is 3D, but with the present model, this 3D problem is split into 2 2D problem (bulk, skin) coupled to optimize the computing time.

This existing TEC3 model has been modified in the present framework to be used both for off-line simulations of rolling campaigns and for on-line calculations with a coil to coil chaining procedure.

The model has also been modified to consider work roll shifting, multiple segmented cooling zones, both across roll barrel length and roll circumference, and composite rolls with different thermal properties in the mandrel and core (Figure 4). Moreover, the thermal crown indicator values C_{40} and C_{100} can be extracted from the model to be compared with existing roll thermal crown models.

2.2 Roll thermal crown evaluation

The roll thermal crown is calculated by the TEC3 model with a 2D thermo-elastic equation without considering the plane strain or plane stress assumptions of Equations (4) and (5) in each y-position:

$$\sigma = 2.\mu.\varepsilon + \lambda.tr\varepsilon.1 - \alpha_T.(2.\mu + 3\lambda).\Delta T.1$$
$$\lambda = \frac{\nu.E}{(1+\nu).(1-2\nu)} \qquad \mu \quad _ \quad E \quad (9)$$

This equation provides higher accuracy in thermal crown prediction for no additional computing time. In practice, the plane stress assumption from literature models gives reasonable approximation of thermal crown in most rolling conditions (Figure 7)

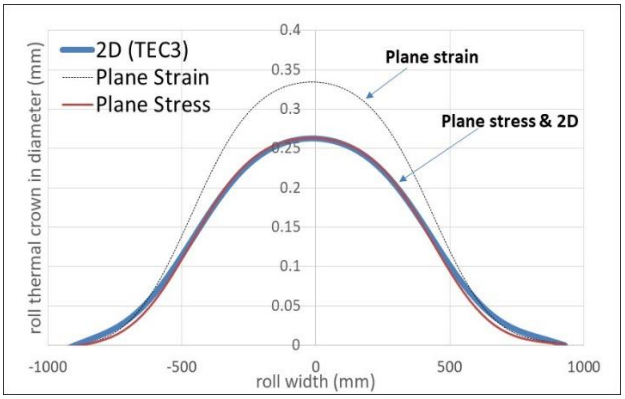

Figure 7. Comparison 2D (TEC3), plane strain and plane stress calculation of thermal crown

2.3 Composite roll analysis

Figure 8 shows roll radial temperature profiles calculated with TEC3 for a homogeneous and a heterogeneous (composite) roll. The composite roll presents a large difference of thermal conductivity K between mandrel and core

of the roll while the homogeneous roll has a uniform conductivity. A knee is observed on the temperature profile at the interface core-mandrel for the composite roll while the profile is smooth (no knee) for the homogeneous roll. The origin of this knee is due to the difference of conductivity core-mandrel: here twice higher in the core (K=34 N/s.k) than in the mandrel (K=17.8 N/s.k), as a consequence the temperature derivative is twice lower:

$$\left(\frac{dT}{dr}\right)_1 = \left(\frac{dT}{dr}\right)_2 /2 \quad (10)$$

to satisfy the continuity of heat flux through the interface core-mandrel:

$$\phi = K.grad(T) = K_{core}.\left(\frac{dT}{dr}\right)_1 = K_{mandrel}.\left(\frac{dT}{dr}\right)_2 \quad (11)$$

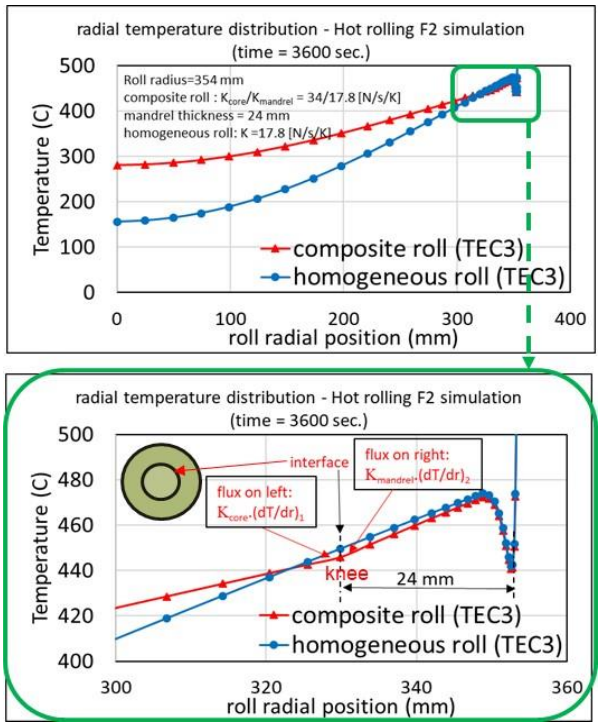

Figure 8. Roll temperature distribution for composite and homogeneous roll – top: complete radial profile, bottom: zoom on the inteface core-mandrel.

Moreover, the thermal contact at the interface core-mandrel is a perfect thermal contact (continuity of temperature and flux).

2.4 Rolls heat transfers analysis

Equations

The roll heat conduction Equations (7) and (8) are linear at first order. Using this linearity, roll heat transfers expressions ϕ and ψ **[8]** illustrated on figure 1 are developed below:

-the total roll bite heat flux ψ can be expressed as a function of the steady state roll temperature T_{eq} and water temperature T_{water} **[8]**:

$$\psi = 2\pi R.h''.(T_{eq} - T_{water}) \quad (12)$$

-the remaining heat flux ϕ of the axi-symmetric model, transferred from the skin to the bulk of the roll is given by **[8]**:

$$\phi = 2\pi R.h'.(T_{eq} - T_s^{axi}) \quad (13)$$

T_{eq}, T_s^{axi} are expressed on figures 1 and 2, h' is the average heat transfer coefficient at the interface skin/bulk of the roll.

The combination of Equations (12) and (13) provides the following equation:

$$\phi = \left(\frac{h'}{h''}\right)\psi - 2\pi R.h'.(T_s^{axi} - T_{water}) \quad (14)$$

Equation (14) expresses that only a partial transfer (h'/h'') of the roll bite heat flux ψ is transferred to the bulk of the roll (usually h'<h'') because the other part of this heat flux has been extracted from the skin area by convection with the external environment (second term of Equation (14)):

$$(T_s^{axi} - T_{water}) = [T(R) - T_{water}] \quad (15)$$

Numerical application:

In this section, a comparison of TEC3 thermal crown model with equivalent homogeneous environment models from literature is presented. For this comparison, h' has been programmed in TEC3.

The simulation conditions of Figure 9 are summarized below:

- roll diameter = 707.9 mm
- strip thickness entry/exit=16.84/10.00 mm
- roll bite heat flux = 60000 kW/m^2
-steady state simulation

Simulation results on figure 9 show that the TEC3 non axi-symmetric model has a speed dependent heat transfer coefficient h' in the bulk area always lower than the average coefficient $\bar{h}$ of the axi-symmetric homogeneous environment model for the whole rolling speed range. The two families of models are identical only for an infinite rolling speed: indeed, when the speed ω is too large, the skin thickness δ becomes near to zero so the model becomes axi-symmetric.

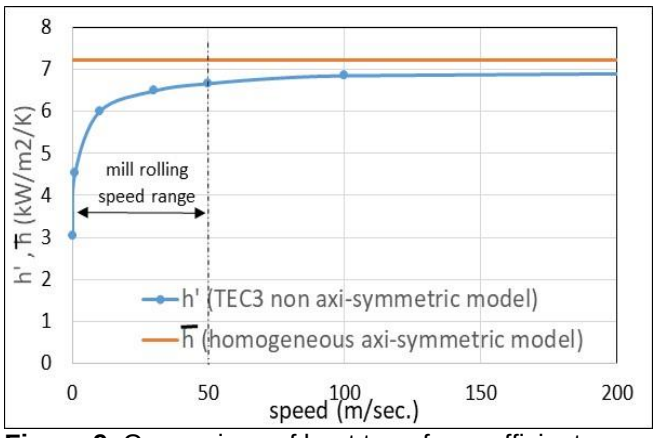

Figure 9. Comparison of heat transfer coefficients: h' from TEC3 versus $\bar{h}$ from equivalent homogeneous environment model.

In addition, a serie of simulations has been carried out in different conditions (change of rolling speed, heat transfer coefficients, roll-coolant and roll conductivity (skin area)). Table 1 shows the range of variation used for each of these parameters while Figure 10 shows the results of these simulations: h' is always lower or equal to $\bar{h}$.

Table 1. factors for the 8192 simulation conditions

Factor	description	range	Number of levels
Ln(speed)	Log of roll linear speed (mm/sec.)	[Ln1000, Ln10000]	4
K	Thermal conductivity in the skin area	[16, 25]	2
	(N/sec./K)		
Ln(h_i)	Ln of heat transfer with cooling zone i (KW/m^2/K)	[Ln1, Ln50]	4
Ln(h_{N+1})	Ln of heat transfer with cooling zone i (KW/m^2/K)	[Ln1, Ln10]	4

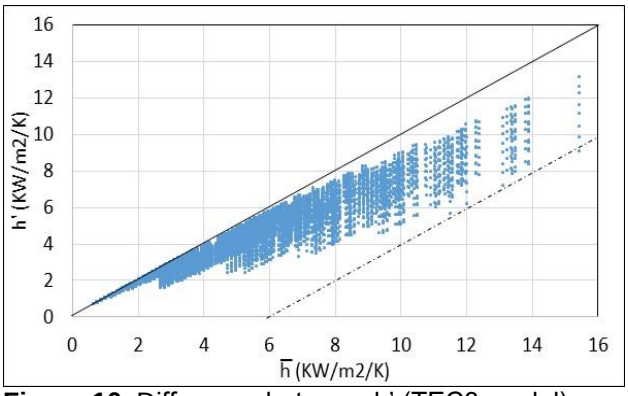

Figure 10. Difference between h' (TEC3 model) and $\bar{h}$ (homogeneous environment model) for the 8192 simulation conditions.

Finally, Table 2 presents the calculations obtained for two different rolling speeds with the TEC3 model. It can be seen that the flux ϕ that penetrates in the center of the roll is higher at larger speed (consequence of the higher h' at larger speed: figure 9). This confirms that the higher the rolling speed is, the lower the roll is cooled.

Table 2. numerical application of h' and h''

Speed (mm/sec.)	h' (kW/m2/K)	h'' (kW/m2/K)	h'/h''	ϕ (W/m)	ψ (W/m)
1000	4.556	11.5	0.396	1.09e6	3.e6
10000	6.0	10.4	0.57	1.51e6	3.e6

From all the above simulation results, It is concluded that the fast temperature evolution in the skin area must be considered by thermal crown models to get accurate heat transfers and thermal crowns calculations. In fact, the present TEC3 model with its boundary conditions (h',ϕ) applied at its axi-symmetric bulk area can describe the influence of rolling speed on roll heat transfers while the literature models with their boundary condition $\bar{h}$ cannot. As a consequence (figure 9),

literature models over-estimate heat transfers between roll and external environment by 10 to 50%, depending on rolling speed.
The origin of this difference is due to the fast skin area: during one roll rotation, roll cooling headers are very efficient at roll gap exit because of the high temperature roll surface temperature. While later in the rotation, the temperature difference [T(R) – T_{water}] is smaller, so roll cooling is less efficient. The h' coefficient from the present model TEC3 includes this continuous change of temperature difference, but not the literature models.

In practice, this skin area is important to consider only if roll-coolant heat transfer coefficients h_i have been measured on roll cooling pilots. However, if these roll-coolant heat transfer coefficients are tuned directly on industrial mills, the purely axi-symmetric models from literature with their $\bar{h}$ can probably be sufficient.

3. TEC3 MODEL CALIBRATION

An optimization methodology to calibrate the tuning parameters of TEC3 model has also been developed. This methodology corresponds to an inverse optimization approach whose main goal is to seek for a set of tuning parameters leading to the smallest difference between experimental measurements and TEC3 numerical results. To do this, the implemented calibration methodology combines an optimization algorithm, responsible for updating the parameters subjected to optimization, with an objective function, responsible for defining the gap between experimental and numerical data and that will control the all optimization process. During the calibration procedure, the tuning parameters set is iteratively updated with the purpose of minimizing the objective function value. Figure 11 depicts the methodology applied to calibrate the TEC3 tuning parameters **[10]**.

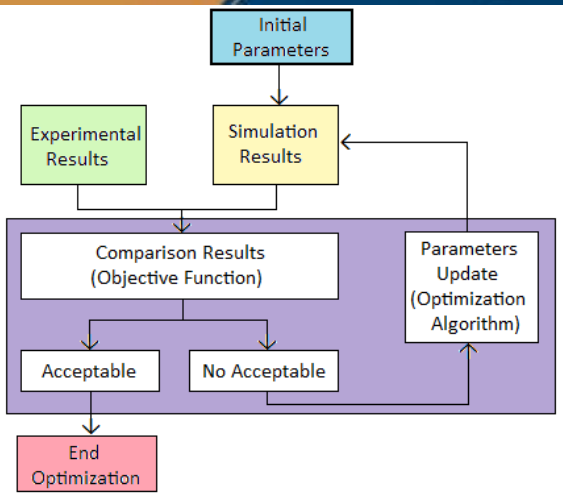

Figure 11. Optimization methodology used to calibrate Tec3 Model.

The objective function plays a crucial role on the model calibration since the optimization process is guided by its minimization, so a suitable definition of the objective function is required. Here, the objective function consists of the sum of the squares of the differences between computed and experimental data:

$$S_{\mathrm{obj}}^{n}(x)=\frac{1}{n_{\mathrm{p}}^{n}}\sum_{i=1}^{n_{\mathrm{p}}^{n}}\left(\frac{Z_i^{\exp}(t_{\mathrm{i}})-Z_i^{\mathrm{num}}(x)}{W_{\mathrm{abs}_k}}\right)^2 \quad (16)$$

where the numerator is the quadratic difference between the experimental $Z_i^{\exp}$ and the numerical Z_i^{num} values for the experimental point *i*, n_p^n stands for the number of points of each experimental test and W_{abs} is a weighting factor that must be normalized according to the different units or scales of the experimental database **[11]**.

3.1 Experiments

The experimental database used in the calibration process is composed by both roll (i) temperature and (ii) thermal crown profiles measured over the work roll barrel length at the end of the rolling campaign. A Pro-Mic device **[12]** and a temperature bar system are generally used to acquire these data as shown in Figure 12.

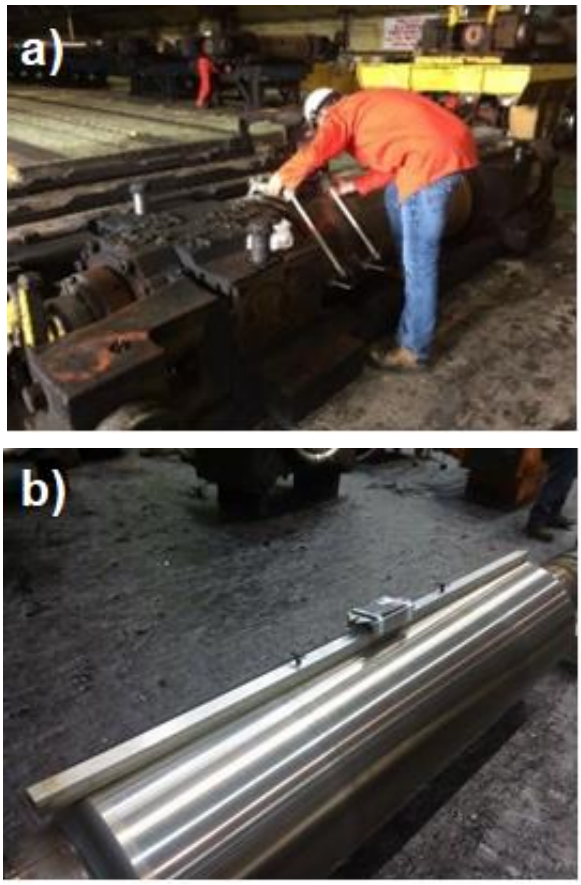

Figure 12. Experimental measurement of the a) roll crown profile using the Pro-Mic device and b) roll temperature profile using temperature bar system.

3.2 Optimization process

The optimization process is conducted by an interface program developed in Matlab. This interface program is linked with the TEC3 model, to perform the numerical simulations, and utilizes the Matlab's optimization toolbox, to update the tuning parameters at each iteration of the optimization process and eventually stop the optimization.

The objective function is minimized using the Levenberg-Marquardt gradient-based algorithm **[13]**. This type of optimization algorithm is characterized (i) by using the information of the derivative of the objective function to successively update the solution and (ii) by a quick convergence in the vicinity of the solution **[11]**.

The tuning parameters subjected to optimization are heat transfer coefficients (HTC): roll bite $\mathbf{HTC_{bite}}$, direct impact coolant jets on roll surface $\mathbf{HTC_{roll\text{-}coolant}}$ and running water around roll surface (excluding direct jets) $\mathbf{HTC_{running\text{-}water}}$.

Constrained parameters optimization is carried out by defining lower and upper bound limits for each tuning parameter. In addition, a maximum number of iterations allowed during the optimization process is also defined.

3.3 Optimization results

The calibraton process has been applied to tune TEC3 model simultaneously on measured roll temperature and thermal crown profiles of ArcelorMittal Dofasco hot strip mill – stand F6. Figure 13 depicts the evolution of the objective function S_{obj} value during the calibration process. By analyzing both starting and final objective function values, it can be observed that a substantial reduction (≈90%) was achieved by the optimization. Such a reduction of the objective function highlights the ability of the optimization algorithm to find a more suitable set of tuning parameters.

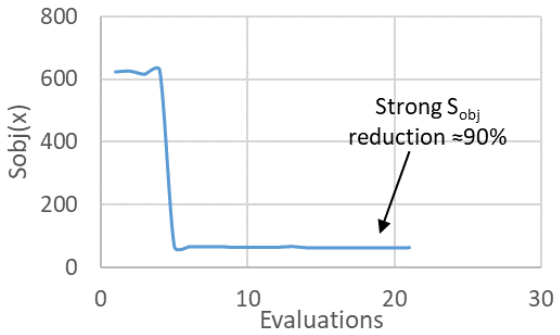

Figure 13. Objective function evolution during the calibration process.

From Figure 14, it can be seen that the initial parameters set leads to a poor reproduction of both the experimental temperature and thermal crown profiles. However, the tuned parameters set found by the optimization process enables a good reproduction of these profiles for this condition. However other conditions (not

shown here) reveal that it might be sometimes difficult to tune the model simultaneously on the two types of measurements (temperature and thermal crown). Further analysis are needed to better understand these difficulties and make the tuning procedure more robust.

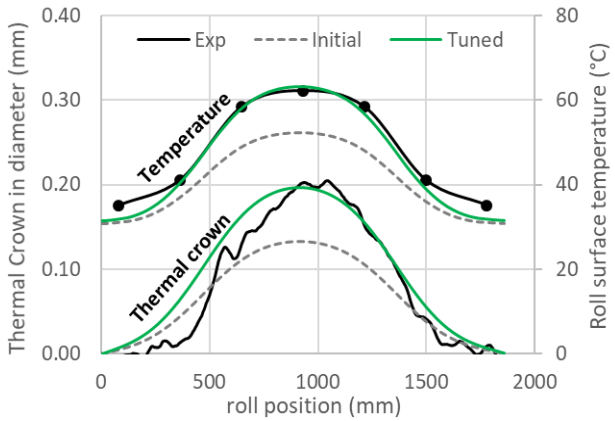

Figure 14. TEC3 calibration results obtained for a rolling campaign of stand F6 of ArcelorMittal Dofasco HSM.

4. TEC3 MODEL APPLICATIONS

4.1 Model application to hot rolling

The Figure 15-a presents thermal crown simulations of real rolling campaigns with TEC3 and Dofasco thermal crown models based on a single crown value calculation C_{40}: the C_{40} of the Dofasco model produces unreal jumps in thermal crown when strip width changes significantly from coil to coil, disturbing the profile and flatness setup calculation. The comparison between C_{40} and C_{100} extracted from the TEC3 thermal crown model shows that a solution to decrease instabilities is to use C_{100} instead of C_{40} in the Dofasco model. A better solution is to develop a model that considers the complete profiles of the rolls and strip (and not considering only a single crown value).

Figure 15-b shows that composite roll properties (thermal conductivity) change thermal crown by ~10% compared to homogeneous roll properties. Moreover, the dissymmetry of thermal crown observed in these results is due to roll shifting.

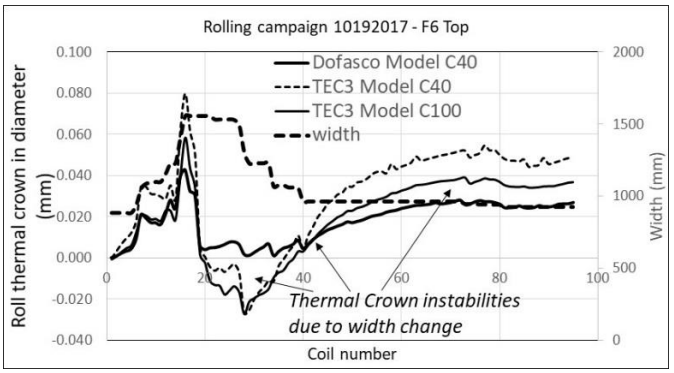

a) comparison TEC3 vs Dofasco thermal crown models

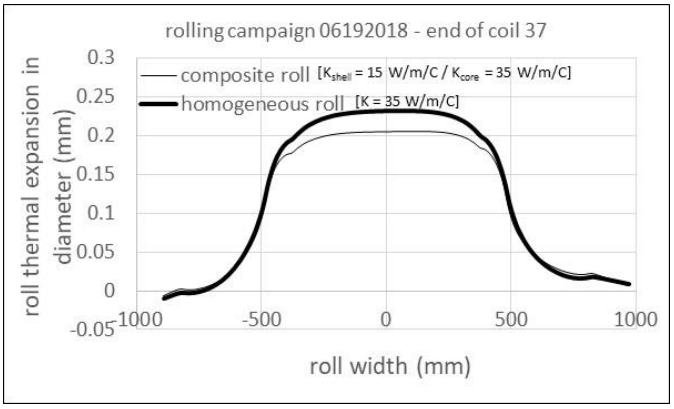

b) composite vs homogeneous roll properties (TEC3)

Figure 15: Simulation results obtained for real hot rolling campaigns.

4.2 Model application to cold rolling

The ArcelorMittal Cleveland 5-stands batch tandem cold mill is equipped with a roll cooling system segmented in 5 different zones: one central zone (C), 2 intermediate zones (I) and 2 external zones (E) both at entry and delivery of the stand. These zones can be opened or closed by operators during rolling to adjust the thermal crown to get a better strip shape control.

Rolling campaigns have been simulated with the TEC3 model for a medium grade rolling campaign. Simulation results presented on figure 16-a highlight the efficiency of this operator's practice. In addition, figure 16-b shows how the temperatures at roll surface, at roll sub-surface and in the center of the roll evolve

as a function of cooling conditions. In particular, it can be observed that during rolling, roll center temperature increases slowly to reach a plateau but is still lower than surface and sub-surface roll temperatures (skin area). While during a long mill stop, roll center temperature becomes slightly higher than the roll skin area temperature (near roll surface).

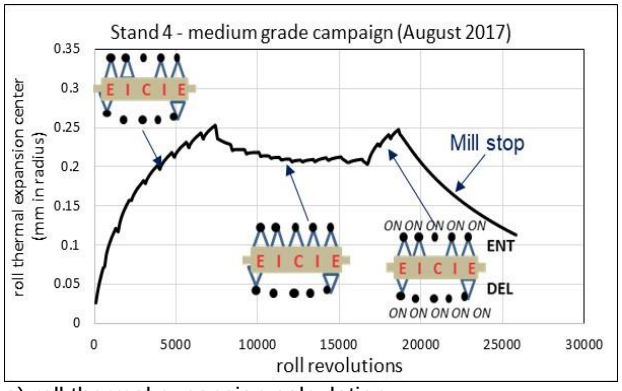

a) roll thermal expansion calculation

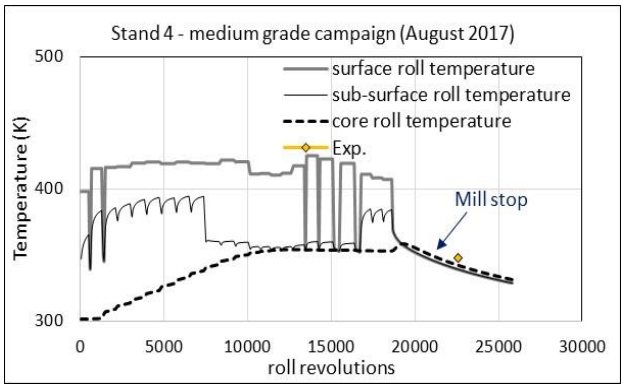

b) roll temperature at surface, at skin/bulk interface and at center

Figure 16: Tec3 thermal simulations for ArcelorMittal Cleveland cold mill

5. CONCLUSION

A comparison was made between two families of thermal crown models: the literature axi-symmetric models considering only the slow temperature evolution in the roll and the TEC3 non axi-symmetric model of the present study that combines fast and slow temperature evolutions in the roll. It is shown that TEC3 can describe the rolling speed dependency of roll heat transfer with environment while the literature models cannot. This gives to TEC3 higher accuracy in roll temperature and thermal crown predictions.

An optimization procedure has been developed to tune the model simultaneously on measured temperature profile and measured thermal crown, application of this procedure reveals sometime the difficulty to tune accurately the model on both type of measurements.

Moreover, TEC3 simulation results in hot rolling show the importance to consider composite rolls properties and their dependency to roll suppliers. Finally, application of the TEC3 model in cold rolling conditions reveals the importance to consider the cooling distribution across the roll length to modify the thermal crown to get better shape control.

Acknowledgments

Pierre Montmitonnet from Cemef laboratory, France is greatly acknowledged for fruitful discussions on thermal crown models.

REFERENCES

1 Bryant, G. F.; Automation of tandem mills (chapter 15), Iron and Steel Institute, 1973.

2 Chefneux, L.; Mignon, J.; Wilmotte, S.; Les variations thermiques du bombé des cylindres d'un train tandem à froid, Commission des Communautés européennes, Report EUR 7755, 1980.

3 Chefneux, L.; Mignon, J.; Wilmotte, S.; Evolution of the working roll cambers during cold rolling, CRM, Metallurgical ECSC Report Nº 58, 1981.

4 Counhaye, C.; Modeling and Industrial Control of Geometry of cold rolled steel strips (in french), PhD thesis, University of Liege, Belgium, 1999.

5 Yamagachi S, Tateno J., Nakata N.; Numerical Analysis of Thermal Expansion of Rolls with Equivalent Transfer Model on Circumference, ISIJ International, Vol. 56 (2006, Nº 12, pp2243-2249

6 Wiklund O. & Al., Profile and flatness methods for rolling of flat products simulated with Mefos's physically based

computer models. 33rd MWSP Conf.Proc., ISS-AIME, Vol XXIX pp.363-369 (1992).

7 Hacquin A., Modelisation Thermomecanique du laminage des produits plats, PhD thesis (in French) (1996).

8 Hacquin A. Coupu J., Developpement d'un nouveau modele de thermique cylindre et integration dans le logiciel CID, ArcelorMittal Internal report (in french), April 2001.

9 Timoshenko, S.; Goodier, J. N.; Theory of Elasticity (pp. 406-410), McGraw-Hill book Co, 1951.

10 Grilo, T.J., Souto, N., Valente, R.A.F., Andrade-Campos, A., Thuillier, S., Sousa, R.J.A., On the development and computational implementation of complex constitutive models and parameters' identification procedures, Key Engineering Materials 554-557, 936-948, 2013.

11 Souto, N., Andrade-Campos, A., Thuillier, S., Material parameter identification within an integrated methodology considering anisotropy, hardening and rupture. JMPT 220, 157-172, 2015.

12 PRO-MIC equipment; https://www.pro-mic.com/PDFs/TN_018.pdf, accessed in 05-2019.

13 Marquardt, D.; An algorithm for least-squares estimation of nonlinear parameters, SIAM Journal on Applied Mathematics 11:431–441, 1963.